

# Non-linear antidamping spin-orbit torque originating from intra-band transport on the warped surface of a topological insulator

Yong-Long Zhou<sup>1</sup>, Hou-Jian Duan<sup>1,2,\*</sup>, Yong-jia Wu<sup>1</sup>, Ming-Xun Deng<sup>1,2</sup>, Lan Wang<sup>4</sup>, Dimitrie Culcer<sup>3</sup>, and Rui-Qiang Wang<sup>1,2†</sup>

<sup>1</sup>Guangdong Provincial Key Laboratory of Quantum Engineering and Quantum Materials, School of Physics and Telecommunication Engineering, South China Normal University, Guangzhou 510006, China

<sup>2</sup>Guangdong-Hong Kong Joint Laboratory of Quantum Matter, Frontier Research Institute for Physics, South China Normal University, Guangzhou 510006, China

<sup>3</sup>School of Physics, The University of New South Wales, Sydney 2052, Australia and

<sup>4</sup>School of Science and ARC Centre of Excellence in Future Low-Energy Electronics Technologies, RMIT Node, RMIT University, Melbourne, VIC 3000, Australia

Motivated by recent experiments observing a large antidamping spin-orbit torque (SOT) on the surface of a three-dimensional topological insulator, we investigate the origin of the current-induced SOT beyond linear-response theory. We find that a strong antidamping SOT arises from intraband transitions in non-linear response, and does not require interband transitions as is the case in linear transport mechanisms. The joint effect of warping and an in-plane magnetization generates a non-linear antidamping SOT which can exceed the intrinsic one by several orders of magnitude, depending on warping parameter and the position of Fermi energy, and exhibits a complex dependence on the azimuthal angle of the magnetization. This nonlinear SOT provides an alternative explanation of the observed giant SOT in recent experiments.

PACS numbers:

Electrical control of magnetic systems has a strong potential for technological applications such as fast magnetic-based storage and computational devices [1]. Recent works in this fast-evolving field have demonstrated that large spin-orbit coupling in ferromagnet/heavy-metal (FM/HM) bilayers can produce strong enough spin-orbit torques (SOTs) to switch the magnetization in the overlayer. Compared to conventional spin transfer torques in ferromagnet/insulator/ferrometal biheterostructures[2, 3], this SOT has a lower current- and energy-threshold required for magnetization switching[4, 5]. In these systems, the antidamping-like (ADL) torque has the same form as the Gilbert damping term in the Landau-Lifshitz-Gilbert equation[6] but has the opposite sign, and competes against Gilbert damping to switch the magnetization. Therefore, a large ADL torque is of particular importance for increasing the efficiency of magnetization switching. Antidamping torques in these structures arise from either the spin Hall effect (SHE) within the bulk of heavy metals[2, 7–11] or the Rashba-Edelstein effect (or the inverse spin galvanic effect) at inversion-symmetry broken interfaces[12–15]. They may also stem from the intrinsic Berry curvature [16], without being related to a bulk SHE.

Besides heavy metals, topological insulators [17, 18], in which the intrinsic strong spin-orbit coupling is large enough to invert the band structure, are the most promising candidates towards efficient transfer of angular momentum between the charge current and the local magnetization. Recent experiments in FM/TI layered structure reported a giant SOT[19–25] even at room temperature. Compared to FM/HM systems the

current density required for magnetization switching[23–26] in FM/TI bilayers is one to two orders of magnitude smaller, and the corresponding effective spin Hall angle[22, 23] is several times larger. Most experiments confirm that the giant SOT originates from the surface states, e.g., the charge-to-spin current conversion efficiency increases when the Fermi energy is within the TI bulk gap rather than in the bulk states [27], excluding contributions from the SHE and Rashba-Edelstein effect. In this context, understanding the origin of the large ADL-SOT in FM/TI bilayers becomes a crucial issue.

Theoretically, there have been many efforts to explain the emergence of large SOTs, especially the antidamping component, at the magnetic surfaces of topological insulators using linear response theory. Garate and Franz[28, 29] ascribed the SOTs in FM/TI bilayers to a topological magnetoelectric effect with emphasis on its dissipationless Hall current for Fermi energies in the Dirac gap. Extending it to finite Fermi energies, this dissipationless damping was also found to arise from intrinsic inter-band transitions[30–33]. Mahfouzi et al.[34] obtained an antidamping torque by considering spin-flip reflection at an interface. Nevertheless major questions remain unanswered. Theoretically[28–33, 35, 36], the ADL-SOT due to the TI surface states has been expressed in the general form  $\tau_D = \tau_d m_z \mathbf{m} \times e\mathbf{E}$  where  $\mathbf{m}$  is a unit magnetization vector and  $\mathbf{E}$  is the electric field. This form does not explain experimental observations: the ADL-SOT is quite weak and vanishes if  $m_z = 0$ , and the in-plane magnetization  $m_{x/y}$  has no effect on the SOT strength  $\tau_d$ . Nevertheless, in many recent experiments on FM/TI bilayers[21, 25], a strong angular dependence of SOTs on the azimuthal angular or  $m_{x/y}$  was widely observed even in the absence of  $m_z$ . Theoretically, it was even doubted that the experimental measurement method relying on the second harmonic Hall voltage could accurately determine the SOT due to the disturbance from asymmetric

\*Electronic address: dhjphd@163.com

†Electronic address: wangruiqiang@m.scnu.edu.cn

magnon scattering[37].

In this Letter, we propose a mechanism for the generation of the ADL-SOT in the nonlinear response regime, purely based on the topological surface states with hexagonal warping, which is strong in realistic TIs[38, 39]. Our work stands in sharp contrast to existing theories, which are exclusively based on linear response. Intriguingly, we find that the nonlinear spin polarization can produce a large ADL-SOT, caused by the interplay between the warping effect and the in-plane magnetization, which is known to have strong observable features in charge transport[40–42]. This non-linear phenomenon is distinguished from previous mechanisms and explains the features of the ADL-SOT observed experimentally.

*Theory for SOT* - The SOT exerted on the FM layer has the form  $\tau = \frac{2J}{\hbar} \mathbf{m} \times \mathbf{S}$  with the spin polarization  $\mathbf{S} = \sum_{\chi} \frac{d^d \mathbf{k}}{(2\pi)^d} \mathbf{s}_{\chi}(\mathbf{k}) f(\varepsilon_{\mathbf{k}}^{\chi})$ , where  $J$  is the  $s$ - $d$  exchange energy, the superscript  $d$  represents the dimension, and  $\mathbf{s}_{\chi}(\mathbf{k}) = (\hbar/2) \langle \Psi_{\mathbf{k}}^{\chi} | \boldsymbol{\sigma} | \Psi_{\mathbf{k}}^{\chi} \rangle$  is the spin expectation in the  $\chi$ -th band with eigenvector  $\Psi_{\mathbf{k}}^{\chi}$  and eigenvalue  $\varepsilon_{\mathbf{k}}^{\chi}$ . In the absence of applied current, the distribution function  $f(\varepsilon_{\mathbf{k}}^{\chi})$  is the Fermi-Dirac distribution function  $f(\varepsilon_{\mathbf{k}}^{\chi}) = f^{(0)}(\varepsilon_{\mathbf{k}}^{\chi}) = [e^{(\varepsilon_{\mathbf{k}}^{\chi} - \varepsilon_F)/k_B T} + 1]^{-1}$  with Fermi energy  $\varepsilon_F$  and temperature  $T$ , and thus  $\mathbf{S}$  vanishes due to  $\mathbf{s}_{\chi}(-\mathbf{k}) = -\mathbf{s}_{\chi}(\mathbf{k})$  for spin-momentum locked surface states of TIs. When an in-plane current is applied, the spin polarization  $\mathbf{S} = \mathbf{S}^{oc} + \mathbf{S}^{in}$  can arise from the two types of change. One originates from the change of the electron occupation  $\delta f(\varepsilon_{\mathbf{k}}^{\chi}) = f(\varepsilon_{\mathbf{k}}^{\chi}) - f^{(0)}(\varepsilon_{\mathbf{k}}^{\chi})$  within intraband due to acceleration by an electric field, calculated by  $\mathbf{S}^{oc} = \sum_{\chi} \frac{d^d \mathbf{k}}{(2\pi)^d} \mathbf{s}_{\chi}(\mathbf{k}) \delta f(\varepsilon_{\mathbf{k}}^{\chi})$ . The other stems from the modification of the quasiparticle wave functions [16, 43, 44],  $\mathbf{S}^{in} = \sum_{\chi} \frac{d^d \mathbf{k}}{(2\pi)^d} \delta \mathbf{s}_{\chi}(\mathbf{k}) f(\varepsilon_{\mathbf{k}}^{\chi})$ , where  $\delta \mathbf{s}_{\chi}(\mathbf{k}) = (\hbar/2) \text{Re} \langle \Psi_{\mathbf{k}}^{\chi} | \boldsymbol{\sigma} | \delta \Psi_{\mathbf{k}}^{\chi} \rangle$  can be traced to the interband contributions in analogy to the intrinsic contribution to the anomalous Hall effect.

We first discuss  $\mathbf{S}^{oc}$  by employing the single-band steady-state Boltzmann equation[45],

$$-\frac{e}{\hbar} \mathbf{E} \cdot \nabla_{\mathbf{k}} f(\varepsilon_{\mathbf{k}}^{\chi}) = -\frac{f(\varepsilon_{\mathbf{k}}^{\chi}) - f^{(0)}(\varepsilon_{\mathbf{k}}^{\chi})}{\gamma(\mathbf{k})}. \quad (1)$$

Here, we use the relaxation time approximation  $\gamma(\mathbf{k}) = \gamma$ . Expanding  $f(\varepsilon_{\mathbf{k}}^{\chi}) = f^{(0)}(\varepsilon_{\mathbf{k}}^{\chi}) + f^{(1)}(\varepsilon_{\mathbf{k}}^{\chi}) + f^{(2)}(\varepsilon_{\mathbf{k}}^{\chi}) + \dots$  with  $f^{(n)}(\varepsilon_{\mathbf{k}}^{\chi}) \propto \mathbf{E}^n$  and then substituting it to the above Boltzmann equation, one can find the recursive relations for  $n$ -th order non-equilibrium distribution function,

$$f^{(n)}(\varepsilon_{\mathbf{k}}^{\chi}) = \frac{e\gamma}{\hbar} \mathbf{E} \cdot \frac{\partial f^{(n-1)}(\varepsilon_{\mathbf{k}}^{\chi})}{\partial \mathbf{k}}. \quad (2)$$

*Nonlinear SOT from intra-band transitions* - We take a FM/TI heterostructure, as shown in Fig. 1, as a sample system exhibiting a spin polarization in response to an applied electric field. On the surface of a three-dimensional TI, the effective Hamiltonian [46, 47] reads

$$H_{TI} = \hbar v_F (\sigma_x k_y - \sigma_y k_x) + \frac{\lambda}{2} (k_+^3 + k_-^3) \sigma_z + \mathbf{J} \mathbf{m} \cdot \boldsymbol{\sigma}, \quad (3)$$

where  $v_F$  is the Fermi velocity,  $\boldsymbol{\sigma} = (\sigma_x, \sigma_y, \sigma_z)$  is the vector of Pauli matrices acting on real spin, and  $k_{\pm} = k_x \pm$

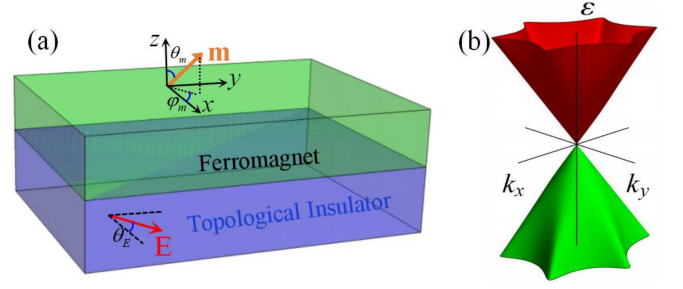


FIG. 1: (a) The FM/TI layered structure, where the orange arrow represents the local magnetic moment with magnetization  $\mathbf{m}$  in the FM layer, and the driven electric field  $\mathbf{E} = (E_x, E_y) = |\mathbf{E}| [\cos(\theta_E), \sin(\theta_E)]$  is applied in the TI layer. (b) Schematics of the band structure for the warped surface states of TIs.

$ik_y$  with  $\mathbf{k}$  being the wave vector. The first term is the Rashba-type spin-orbit coupling, the cubic-in- $\mathbf{k}$  term represents the hexagonal warping effect[38, 39] of TIs with the warping parameter  $\lambda$ , and the FM layer is characterized by a local magnetization  $\mathbf{m} = (m_x, m_y, m_z) = [\sin(\theta_m) \cos(\varphi_m), \sin(\theta_m) \sin(\varphi_m), \cos(\theta_m)]$ . The energy dispersion of the Hamiltonian in Eq. (3) reads

$$\varepsilon_{\mathbf{k}}^{\chi} = \chi \hbar v_F \sqrt{(k_x - Jm_y/\hbar v_F)^2 + (k_y + Jm_x/\hbar v_F)^2 + \Lambda_{\mathbf{k}}^2}, \quad (4)$$

where  $\Lambda_{\mathbf{k}} = [\lambda k_x (k_x^2 - 3k_y^2) + Jm_z]/(\hbar v_F)$  and  $\chi = \pm$  are the upper and lower bands. Notice that the in-plane magnetization  $m_{x/y}$  on the dispersion cannot be eliminated by performing a gauge transformation due to the existence of the warping term.

In linear response, we retain the non-equilibrium distribution function up to the first order  $f^{(1)}(\varepsilon_{\mathbf{k}}^{\chi})$  and calculate the linear polarization  $\mathbf{S}^{oc(1)} = \sum_{\chi} \frac{d^d \mathbf{k}}{(2\pi)^d} \mathbf{s}_{\chi}(\mathbf{k}) f^{(1)}(\varepsilon_{\mathbf{k}}^{\chi})$ . We find that  $\mathbf{S}^{oc(1)}$  only contributes to the field-like SOT (FL-SOT) and no antidamping SOT arises even for the case with strong warping (see Supplement materials[48] or our previous work[49]). Here, extending the theory to the nonlinear one, we calculate the non-linear spin polarization with  $\mathbf{S}^{oc(2)} = \sum_{\chi} \frac{d^d \mathbf{k}}{(2\pi)^d} \mathbf{s}_{\chi}(\mathbf{k}) f^{(2)}(\varepsilon_{\mathbf{k}}^{\chi})$ . We assume the Fermi level  $\varepsilon_F > 0$  lies in the upper surface-band  $\chi = 1$  and the band index is suppressed afterwards. Choosing the in-plane electric field  $\mathbf{E} = (E_x, E_y)$ , at low temperatures we obtain the analytical expressions for the nonlinear spin polarization

$$\begin{aligned} S_x^{oc(2)} &= C \left[ a_2 m_x E_y^2 + (a_1 m_z - a_2 m_y) E_x E_y \right], \\ S_y^{oc(2)} &= C \left[ \left( \frac{a_1 m_z}{2} + a_2 m_y \right) E_x^2 - \frac{a_1 m_z}{2} E_y^2 - a_2 m_x E_x E_y \right], \\ S_z^{oc(2)} &= C \left[ \left( \frac{3}{2} a_1 m_y - a_0 m_z \right) E_x^2 - \left( a_0 m_z + \frac{3}{2} a_1 m_y \right) E_y^2 \right. \\ &\quad \left. + 3C a_1 m_x E_x E_y \right], \end{aligned} \quad (5)$$

where we retain up to the second-order term of  $\mathbf{m}$  and  $\lambda$ , and denote  $C = e^2 \gamma^2 v_F J / (8\pi)$ ,  $a_0 = 1/(\hbar v_F \varepsilon_F)$ ,  $a_1 = 3\lambda \varepsilon_F / (\hbar^4 v_F^4)$ , and  $a_2 = 3\lambda^2 \varepsilon_F^3 / (\hbar^7 v_F^7)$ .

Interestingly, unlike the even function of  $\mathbf{m}$  appearing in linear response, the nonlinear spin polarizations in Eq. (5)

are odd functions of  $\mathbf{m}$  while all the second-order terms in  $\mathbf{m}$  disappear. Thus, the nonlinear spin polarization contributes an antidamping SOT  $\tau_D^{oc} = \frac{2J}{\hbar} \mathbf{m} \times \mathbf{S}^{oc(2)}$  with strength  $\tau_d^{oc} = \frac{2J}{e\hbar|\mathbf{E}|} |\mathbf{S}^{oc(2)}|$ . This result is unexpected since the change in the electron occupation on the Fermi surface usually only contributes to the FL-SOT. In FM/HM or FM/TI bilayer, the existing mechanisms for the antidamping SOT include the contribution from the Berry curvature[5, 16] or the electric-field-induced intrinsic interband transition[31–33, 49, 50] or extrinsic disorder-induced interband-coherence effects[43]. There are also some emerging new mechanisms such as interface spin currents[51], spin anomalous Hall effect[52], nonreciprocal generation of spin current[53], planar Hall current[54], and magnon[55]. These mechanisms are based on the linear response theory. Here, we propose an alternative mechanism only associated with the intraband transitions beyond linear response theory.

In order to illustrate the role of the warping effect, we set  $\lambda = 0$ , and Eq. (5) reduces to  $S_z^{oc(2)} = \frac{-e^2\gamma^2 v_F J}{8\pi} a_0 m_z |\mathbf{E}|^2$ , which is controlled only by  $m_z$  and proportional to  $1/\varepsilon_F$ , and the other components vanish. This implies that the linear- $\mathbf{k}$  Dirac dispersion also can give rise to a non-linear spin polarization, which is distinct from the electric field-induced nonlinear current[40, 41] where the current  $\mathbf{j} \propto \lambda$ . Thus the current-spin correspondence fails in the non-linear regime even in the absence of warping. For finite warping  $\lambda \neq 0$ , not only  $m_z$  but also the in-plane magnetization  $m_{x/y}$  play a role. Besides modifying the magnitude of  $S_z^{oc(2)}$ ,  $m_{x/y}$  also generate extra in-plane components  $S_{x/y}^{oc(2)}$ . Importantly, all of warping-related components are proportional to  $\varepsilon_F$  and  $\lambda$  or their higher orders. We calculate the numerical result of  $\tau_d^{oc}$  directly with  $\mathbf{S}^{oc(2)} = \int \frac{d^2\mathbf{k}}{(2\pi)^2} \mathbf{s}(\mathbf{k}) f^{(2)}(\mathbf{k})$  rather than with the analytical expressions Eq. (5), and present the numerical result of  $\tau_d^{oc}$  as a function of  $\lambda$  in Fig. 2(a), where all parameters are within the range of realistic TI materials. Prominently, the resulting ADL-SOT  $\tau_d^{oc}$  strength increases remarkably as  $\lambda$  or  $\varepsilon_F$  increases. Therefore, for large  $\varepsilon_F$  and  $\lambda$ ,  $\tau_d^{oc}$  can be enhanced significantly in comparison with the case of Refs.[31–33, 49] in absence of warping. In addition,  $\tau_d^{oc}$  exhibits a complex dependence on the azimuthal angle of  $\mathbf{m}$ , as shown in Fig. 2(b). A complex angular dependence of the SOT has been observed in recent experimental measurements in TI bilayers [20–22, 25] but has not been explained theoretically to date.

*Understanding of intraband nonlinear damping SOT-* For the linear Dirac case ( $\lambda = 0$ ), a current-spin correspondence  $\hat{v} = v_F \hat{z} \times \sigma$  can be established due to spin-momentum locking, and then nonequilibrium spin polarization reads  $\mathbf{S} = -\frac{1}{e v_F} \hat{z} \times \mathbf{j}$ . Here, the longitudinal conductance contributes to the FL-SOT and the transversal conductance contributes to the damping-like SOT. This correspondence relation is satisfied only for linear spin polarization without  $\lambda$  and is broken by warping [49]. In the non-linear case, even for  $\lambda = 0$ , the correspondence is not followed since  $S_z^{oc(2)} = \frac{e^2\gamma^2 v_F J}{8\pi} a_0 m_z |\mathbf{E}|^2$  but  $\mathbf{j} \propto \lambda$  vanishes (see Section B of the supplementary material[48]). Thus, we cannot simply attribute the non-linear spin polarization to the non-linear longitudinal or transverse conductance.

When applying an electric field on the TI surface, the

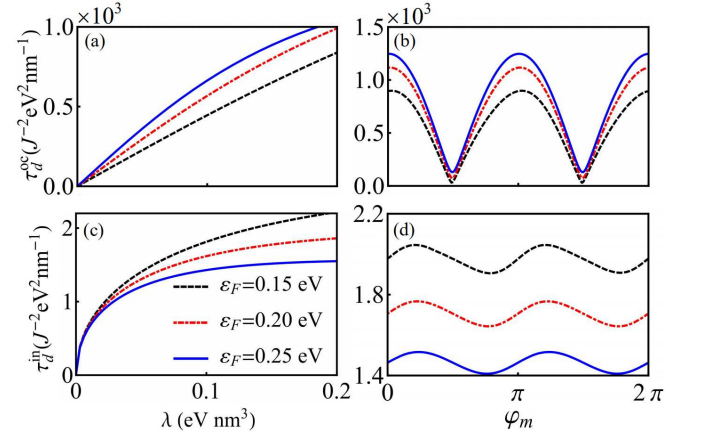


FIG. 2: Dependence of the strength of SOT (a)  $\tau_d^{oc}$  and (c)  $\tau_d^{in}$  on the warping parameter  $\lambda$  with constant azimuthal angle of  $\mathbf{m}$  ( $\varphi_m = \pi/4$ ) for different Fermi energies. (b) and (d) The  $\varphi_m$ -dependent strength of SOT with constant  $\lambda = 0.15 \text{ eV} \cdot \text{nm}^3$ . Other parameters are set as:  $\theta_m = \pi/2$ ,  $\theta_E = \pi/4$ ,  $v_F = 5 \times 10^5 \text{ m/s}$ ,  $\gamma = 3 \text{ ps}$ , and  $|\mathbf{E}| = 0.2 \text{ mV/nm}$ .

hexagonal warped Fermi surface would shift in  $\mathbf{k}$ -space, and generates a net linear spin accumulation due to the spin-momentum locking, as given by the  $\mathbf{m}$ -independent term in Eq. (A.7) of supplementary materials[48]. However, this shift cannot generate a non-linear spin accumulations as given in Eq. (5), where all terms are related to the magnetization  $\mathbf{m}$ . In order to understand the generation of the nonlinear spin polarization, we need to analyze the symmetry of the integrand in  $\mathbf{S}^{oc(2)} = \int \frac{d^2\mathbf{k}}{(2\pi)^2} \mathbf{s}(\mathbf{k}) f^{(2)}(\mathbf{k})$ . In the absence of the magnetization, the average spin  $\mathbf{s}(\mathbf{k})$  is odd in  $\mathbf{k}$  whereas the second-order distribution function  $f^{(2)}(\mathbf{k})$  is even in  $\mathbf{k}$ . As a consequence,  $\mathbf{S}^{oc(2)} = 0$ .

When  $\mathbf{m}$  is introduced, however, the warped Fermi surface is further distorted except for the shift, which not only changes the occupation of the electron states but also perturbs the spin textures, giving an additional deviation to the spin direction at each  $\mathbf{k}$ -point. In this case, both  $\mathbf{s}(\mathbf{k})$  and  $f^{(2)}(\mathbf{k})$  have symmetric and asymmetric components with respect to  $\mathbf{m}$ . Up to second-order in  $J$  or  $\mathbf{m}$  (see Section C of the supplementary materials[48]), we expand  $\mathbf{s}(\mathbf{k}) = \sum_{i=0,1,2} s^i(\mathbf{k}) J^i$  and  $f^{(2)}(\mathbf{k}) = \sum_{i=0,1,2} f_i^{(2)} J^i$ . It is easy to check that  $s^i(\mathbf{k})$  is odd and  $f_i^{(2)}$  is even in  $\mathbf{k}$  for  $i = 0, 2$ , while  $s^i(\mathbf{k})$  is even and  $f_i^{(2)}$  is odd for  $i = 1$ . Thus, the nonzero integrand terms of  $\mathbf{k}$  in  $\mathbf{S}^{oc(2)}$  are  $s^0(\mathbf{k}) \cdot f_1^{(2)}(\mathbf{k})$  and  $s^1(\mathbf{k}) \cdot f_0^{(2)}(\mathbf{k})$ . In Fig. 3, we plot the variation of the second-order correction  $f_i^{(2)}$  of the distribution function along the  $\mathbf{k}$ -axis parallel to the applied electric field  $\mathbf{E}$ . In the absence of  $\mathbf{m}$  as in Figs. 3(a), the occupations of the electron states at  $\mathbf{k}$  and  $-\mathbf{k}$  are the same but the corresponding spins are opposite, which contributes no net spin polarization. Once a nonzero  $\mathbf{m}$  is introduced, the component  $f_1^{(2)}(\mathbf{k})$  of the occupation or  $s^1(\mathbf{k})$  change parity. In Fig. 3(b) where both  $f_1^{(2)}(\mathbf{k})$  and  $s^0(\mathbf{k})$  are odd, the down-spin electrons are depleted while the up-spin ones are in excess, which makes the opposite spins carried by the electrons in  $\mathbf{k}$  and  $-\mathbf{k}$  cannot cancel each other, and so a net nonlinear spin polarization

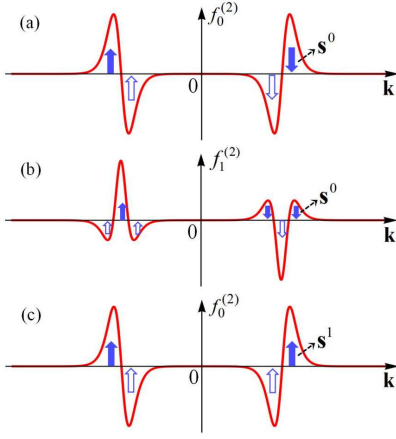


FIG. 3: Schematics of variation of the second-order correction  $f_i^{(2)}$  of the distribution function along the  $\mathbf{k}$ -axis parallel to the applied electric field  $\mathbf{E}$ . Blue solid arrows represent excess of electrons with spins along the arrow direction, and hollow arrows represent depletion of the same. (a) describes the vanishing contribution from the component  $\mathbf{s}^0(\mathbf{k}) \cdot f_0^{(2)}(\mathbf{k})$ . The nonzero polarization stemming from the components (b)  $\mathbf{s}^0(\mathbf{k}) \cdot f_1^{(2)}(\mathbf{k})$  and (c)  $\mathbf{s}^1(\mathbf{k}) \cdot f_0^{(2)}(\mathbf{k})$ .

appears for  $\mathbf{s}^0(\mathbf{k}) \cdot f_1^{(2)}(\mathbf{k})$ . Compared with Fig. 3(a), this is a result of  $f^{(2)}(\mathbf{k})$  changing from even to odd function, namely,  $f_0^{(2)}(\mathbf{k}) \rightarrow f_1^{(2)}(\mathbf{k})$ , by the interplay of the magnetization and the nontrivial spin texture of warping effect. Fig. 3(c) describes the case of  $\mathbf{s}^1(\mathbf{k}) \cdot f_0^{(2)}(\mathbf{k})$ , where the even  $f^{(2)}(\mathbf{k})$  keeps the same, compared with Fig. 3(a), but  $\mathbf{s}(\mathbf{k})$  is changed from odd to even function  $\mathbf{s}^0(\mathbf{k}) \rightarrow \mathbf{s}^1(\mathbf{k})$ .  $\mathbf{s}^1(-\mathbf{k}) = \mathbf{s}^1(\mathbf{k})$  means the same spin orientations at  $\mathbf{k}$  and  $-\mathbf{k}$ , which mainly originate from the deviation of out-of-plane spin in warping effect by the magnetization or by out-of-plane  $m_z$ . The latter contributes  $S_z^{oc(2)} \propto a_0 m_z$ , which will quickly shrink for the Fermi energy away from the Dirac point due to  $a_0 \propto \frac{1}{\varepsilon_F}$ . Physically, the distortion of Fermi surface leads to change of spin texture and unequal population of electrons with opposite momenta as well as spins and so generates the nonlinear spin polarization. The increasing parameter  $\lambda$  will enhance the distortion effect and then the nonlinear spin polarization.

*Comparison of nonlinear SOT with intrinsic SOT-* It is interesting to compare the non-linear antidamping SOT with that from the Berry curvature caused by intrinsic interband transitions,  $\mathbf{S}^{in} = \sum_{\chi \neq \chi'} \frac{d^d \mathbf{k}}{(2\pi)^d} \delta \mathbf{s}_{\chi}(\mathbf{k}) f(\varepsilon_{\mathbf{k}}^{\chi})$ , where  $\delta \mathbf{s}_{\chi}(\mathbf{k}) = (\hbar/2) \text{Re} \langle \Psi_{\mathbf{k}}^{\chi} | \boldsymbol{\sigma} | \delta \Psi_{\mathbf{k}}^{\chi} \rangle$ . By modifying the quasiparticle wave functions  $|\delta \Psi_{\mathbf{k}}^{\chi}\rangle$  with perturbation method, the spin polarization is given by[16, 43, 44],

$$\mathbf{S}^{in} = \frac{e\hbar^2}{V} \sum_{\chi \neq \chi', \mathbf{k}} [f(\varepsilon_{\mathbf{k}}^{\chi}) - f(\varepsilon_{\mathbf{k}}^{\chi'})] \frac{\text{Im} \left[ \langle \Psi_{\mathbf{k}}^{\chi} | \boldsymbol{\sigma} | \Psi_{\mathbf{k}}^{\chi'} \rangle \langle \Psi_{\mathbf{k}}^{\chi'} | \hat{\mathbf{v}} \cdot \mathbf{E} | \Psi_{\mathbf{k}}^{\chi} \rangle \right]}{(\varepsilon_{\mathbf{k}}^{\chi} - \varepsilon_{\mathbf{k}}^{\chi'})^2} \quad (6)$$

This expression is analogous to the intrinsic Berry curvature mechanism originally introduced to explain the anomalous Hall effect[56] and the SHE[57] due to the electric-field-induced interband-coherence. It is found that this antidamp-

ing Berry-curvature SOT can contribute with a strength comparable to that of the SHE-driven antidamping torque, and has given good explanation for ADL-SOT experiments with Rashba-model ferromagnets[16].

Here, we apply this intrinsic Berry curvature mechanism to the FM/TI bilayer. For  $\lambda = 0$ , we obtain  $S_z^{in} = 0$  and

$$S_{x/y}^{in} = \frac{e\hbar J}{8\pi} a_0 m_z E_{x/y}. \quad (7)$$

Obviously, only  $m_z$  contributes to the spin polarization and in turn the intrinsic damping SOT, which recalls the results of Ref.[28, 30–33, 35] based on the Green's function Kubo formula. For  $\lambda \neq 0$ ,  $m_{x/y}$  also play a role for the intrinsic damping. In view of the complex analytical expressions we only present the numerical results  $\tau_d^{in} = \frac{2J}{e\hbar|\mathbf{E}|} |\mathbf{S}^{in}|$  in Figs. 2(c) and (d).

We compare the non-linear SOT strength  $\tau_d^{oc}$  in Figs. 2(a)-(b) to the Berry-curvature SOT strength  $\tau_d^{in}$  in Figs. 2(c)-(d). One can find that: (I) While  $\tau_d^{in}$  slightly increases with the warping parameter  $\lambda$ ,  $\tau_d^{oc}$  increases quickly. (II) As  $\varepsilon_F$  increases,  $\tau_d^{oc}$  increases while  $\tau_d^{in}$  decreases. Thus, Figure 2 shows that  $\tau_d^{oc}$  is larger than  $\tau_d^{in}$  by two to three orders of magnitude for chosen parameters, which are in the range of realistic materials. In practice, the applied electric field strength in FM/TI SOT experiments[23–25] is estimated as  $|\mathbf{E}| = 0.1\text{--}0.3$  mV/nm, the relaxation time in the TI Bi<sub>2</sub>Se<sub>3</sub> is typically[58]  $\gamma = 3$  ps, and the warping parameter[41, 59] is  $\lambda = 0.056\text{--}0.18$  eV · nm<sup>3</sup>. In addition, different from  $\tau_d^{in}$ ,  $\tau_d^{oc}$  shows the more complicate angular dependence on  $\mathbf{m}$ , compared Figs. 2(b) with (d).

Owing to the warping effect, the current-induced SOT depends on the current direction. In order to clarify the current-induced anisotropy of the SOT, we plot  $\tau_d^{oc}$  and  $\tau_d^{in}$  as a function of the direction of the electric field  $\theta_E$  in Figs. 4 (a) and (b), respectively. Obviously, the ADL-SOTs are isotropic for  $\lambda = 0$  and anisotropic for  $\lambda \neq 0$ , the larger the warping parameter (or Fermi energy), the more obvious the anisotropy is. More importantly, the periods of these two kinds of SOTs are significantly different, which could lead to an enhanced ratio  $\tau_d^{oc}/\tau_d^{in}$  for a certain current direction  $\theta_E$ .

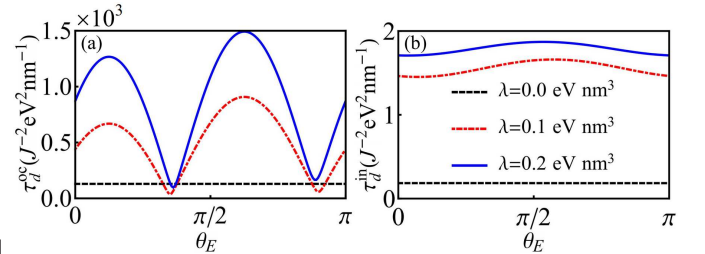


FIG. 4: The strength of SOT (a)  $\tau_d^{oc}$  and (b)  $\tau_d^{in}$  with respect to the current direction  $\theta_E$  for different warping parameters. Parameters are set as  $\varepsilon_F = 0.2\text{eV}$ ,  $\theta_m = 19\pi/40$ , and  $\varphi_m = \pi/4$ . Other parameters are the same as in Fig. 2.

*Conclusion-* We have studied the current-induced nonlinear spin polarization and SOT in a FM/TI bilayer with hexagonal

warping. We focus on the single-band case by employing the Boltzmann equation, and find that the nonlinear spin polarization associated with intraband transitions generates a strong ADL-SOT, unlike the spin polarization linear in the electric field, which only contributes to the FL-SOT. The non-linear antidamping SOT not only stems from the out-plane magnetization  $m_z$ , but also from the joint effect of warping and in-plane magnetizations  $m_x$  and  $m_y$ . The present mechanism is associated with intraband transitions, distinguished from the existing linear-response theory[5, 16, 31–33, 43, 49, 50], where inter-band transitions are necessary. More importantly, the non-linear ADL-SOT is enhanced with increasing Fermi energy and warping parameter, and can be several orders of magnitude larger than that of the intrinsic Berry-curvature contributions. It exhibits a complex dependence on the azimuthal angle of the magnetization, which is consistent with experiment. This nonlinear SOT provides a new mechanism

for the explanation of the giant SOT in recent experiments.

### Acknowledgments

This work was supported by GDUPS (2017), by the National Natural Science Foundation of China (Grants No. 12174121, No. 11904107, and No. 12104167), by the Guangdong NSF of China (Grants No. 2021A1515010369 and No. 2020A1515011566), by Guangdong Basic and Applied Basic Research Foundation (Grant No. 2020A1515111035). DC is supported by the Australian Research Council Future Fellowship FT190100062. LW is supported by the Australian Research Council Centre of Excellence in Future Low-Energy Electronics Technologies CE170100039.

- 
- [1] I. Žutić, J. Fabian, and S. D. Sarma, *Rev. Mod. Phys.* **76**, 323 (2004).
- [2] A. Manchon, J. Železný, I. M. Miron, T. Jungwirth, J. Sinova, A. Thiaville, K. Garello, and P. Gambardella, *Rev. Mod. Phys.* **91**, 035004 (2018).
- [3] G. Prenat, K. Jabeur, G. D. Pendina, O. Boulle, G. Gaudin, W. Zhao, and G. Prenat, *Springer*, 145 (2015).
- [4] G. Prenat, K. Jabeur, P. Vanhauwaert, G. D. Pendina, F. Oboril, R. Bishnoi, M. Ebrahimi, N. Lamard, O. Boulle, K. Garello, J. Langer, B. Ocker, M.-C. Cyrille, P. Gambardella, M. Tahoori, and G. Gaudin, *IEEE Trans. Multi-Scale Computing Systems* **2**, 49 (2016).
- [5] K.-S. Lee, D. Go, A. Manchon, P. M. Haney, M. D. Stiles, H.-W. Lee, and K.-J. Lee, *Phys. Rev. B* **91**, 144401 (2016).
- [6] T. Yokoyama, *Phys. Rev. B* **84**, 113407 (2011).
- [7] L. Liu, C.-F. Pai, Y. Li, H. W. Tseng, D. C. Ralph, and R. A. Buhrman, *Science* **336**, 555 (2012).
- [8] L. Liu, O. J. Lee, T. J. Gudmundsen, D. C. Ralph, and R. A. Buhrman, *Phys. Rev. Lett.* **109**, 096602 (2012).
- [9] L. Liu, C.-F. Pai, D. C. Ralph, and R. A. Buhrman, *Phys. Rev. Lett.* **109**, 186602 (2012).
- [10] J. Sinova, S. O. Valenzuela, J. Wunderlich, C. H. Back, and T. Jungwirth, *Rev. Mod. Phys.* **87**, 1213 (2015).
- [11] J. Sinova and T. Jungwirth, *Phys. Today* **70**, 38 (2017).
- [12] M. Trushin and J. Schliemann, *Phys. Rev. B* **75**, 155323 (2007).
- [13] I. M. Miron, T. Moore, H. Szabolcs, L. D. Buda-Prejbeanu, S. Auffret, B. Rodmacq, S. Pizzini, J. Vogel, M. Bonfim, A. Schuhl, and G. Gaudin, *Nat. Mater.* **10**, 419 (2011).
- [14] T. D. Skinner, K. Olejník, L. K. Cunningham, H. Kurebayashi, R. P. Campion, B. L. Gallagher, T. Jungwirth, and A. J. Ferguson, *Nat. Commun.* **6**, 6730 (2015).
- [15] L. Chen, M. Gmitra, M. Vogel, R. Islinger, M. Kronseder, D. Schuh, D. Bougeard, J. Fabian, D. Weiss, and C. H. Back, *Nat. Electron.* **1**, 350 (2018).
- [16] H. Kurebayashi, J. Sinova, D. Fang, A. C. Irvine, T. D. Skinner, J. Wunderlich, V. Novák, R. P. Campion, B. L. Gallagher, E. K. Vehstedt, L. P. Žárbo, K. Výborný, A. J. Ferguson, and T. Jungwirth, *Nat. Nanotechnol.* **9**, 211 (2014).
- [17] M. Z. Hasan and C. L. Kane, *Rev. Mod. Phys.* **82**, 3045 (2010).
- [18] X.-L. Qi and S.-C. Zhang, *Rev. Mod. Phys.* **83**, 1057 (2011).
- [19] Y. Wang, P. Deorani, K. Banerjee, N. Koirala, M. Brahlek, S. Oh, and H. Yang, *Phys. Rev. Lett.* **114**, 257202 (2015).
- [20] Y. Fan, X. Kou, P. Upadhyaya, Q. Shao, L. Pan, M. Lang, X. Che, J. Tang, M. Montazeri, K. Murata, L.-T. Chang, M. Akyol, G. Yu, T. Nie, K. L. Wong, J. Liu, Y. Wang, Y. Tserkovnyak, and K. L. Wang, *Nat. Nanotechnol.* **11**, 352 (2016).
- [21] A. R. Mellnik, J. S. Lee, A. Richardella, J. L. Grab, P. J. Mintun, M. H. Fischer, A. Vaezi, A. Manchon, E.-A. Kim, N. Samarth, and D. C. Ralph, *Nature* **511**, 449 (2014).
- [22] Y. Fan, P. Upadhyaya, X. Kou, M. Lang, S. Takei, Z. Wang, J. Tang, L. He, L.-T. Chang, M. Montazeri, G. Yu, W. Jiang, T. Nie, R. N. Schwartz, Y. Tserkovnyak, and K. L. Wang, *Nat. Mater.* **13**, 699 (2014).
- [23] J. Han, A. Richardella, S. A. Siddiqui, J. Finley, N. Samarth, and L. Liu, *Phys. Rev. Lett.* **119**, 077702 (2017).
- [24] Y. Wang, D. Zhu, Y. Wu, Y. Yang, J. Yu, R. Ramaswamy, R. Mishra, S. Shi, M. Elyasi, K.-L. Teo, Y. Wu, and H. Yang, *Nat. Commun.* **8**, 1364 (2017).
- [25] D.C. Mahendra, R. Grassi, J.-Y. Chen, M. Jamali, D. R. Hickey, D. Zhang, Z. Zhao, H. Li, P. Quarterman, Y. Lv, M. Li, A. Manchon, K. A. Mkhoyan, T. Low, and J.-P. Wang, *Nat. Mater.* **17**, 800 (2018).
- [26] C. H. Li, O. M. J. van't Erve, S. Rajput, L. Li, and B. T. Jonker, *Nat. Commun.* **7**, 13518 (2016).
- [27] M. Mogi, K. Yasuda, R. Fujimura, R. Yoshimi, N. Ogawa, A. Tsukazaki, M. Kawamura, K. S. Takahashi, M. Kawasaki, and Y. Tokura, *Nat. Commun.* **12**, 1404 (2021).
- [28] I. Garate and M. Franz, *Phys. Rev. Lett.* **104**, 146802 (2010).
- [29] D. Kurebayashi and N. Nagaosa, *Phys. Rev. B* **100**, 134407 (2019).
- [30] P. B. Ndiaye, C. A. Akosa, M. H. Fischer, A. Vaezi, E.-A. Kim, and A. Manchon, *Phys. Rev. B* **96**, 014408 (2017).
- [31] T. Yokoyama, J. Zang, and N. Nagaosa, *Phys. Rev. B* **81**, 241410 (2010).
- [32] T. Chiba, S. Takahashi, and G. E. W. Bauer, *Phys. Rev. B* **95**, 094428 (2017).
- [33] A. Sakai and H. Kohno, *Phys. Rev. B* **89**, 165307 (2014).
- [34] F. Mahfouzi, B. K. Nikolić, and N. Kioussis, *Phys. Rev. B* **93**, 115419 (2015).
- [35] T. Chiba and T. Komine, *Phys. Rev. Appl.* **14**, 034031 (2020).
- [36] T. Gao, A. Qaiumzadeh, H. An, A. Musha, Y. Kageyama, J. Shi, and K. Ando, *Phys. Rev. Lett.* **121**, 017202 (2018).

- [37] K. Yasuda, A. Tsukazaki, R. Yoshimi, K. Kondou, K. S. Takahashi, Y. Otani, M. Kawasaki, and Y. Tokura, *Phys. Rev. Lett.* **119**, 137204 (2017).
- [38] R. S. Akzyanov and A. L. Rakhmanov, *Phys. Rev. B* **97**, 075421 (2018).
- [39] R. S. Akzyanov and A. L. Rakhmanov, *Phys. Rev. B* **99**, 045436 (2019).
- [40] S.S.L. Zhang and G. Vignale, in *Proc. SPIE* **10732**, 1073215 (2018).
- [41] P. He, S. S.-L. Zhang, D. Zhu, Y. Liu, Y. Wang, J. Yu, G. Vignale, and H. Yang, *Nat. Phys.* **14**, 495 (2018).
- [42] P. Bhalla, A.H. MacDonald, and D. Culcer, *Phys. Rev. Lett.* **124**, 087402 (2020).
- [43] C. Xiao and Q. Niu, *Phys. Rev. B* **96**, 045428 (2017).
- [44] I. Garate and A. H. MacDonald, *Phys. Rev. B* **80**, 134403 (2009).
- [45] C.-X. Liu, X.-L. Qi, H. Zhang, X. Dai, Z. Fang, and S.-C. Zhang, *Phys. Rev. B* **82**, 045122 (2010).
- [46] Y. L. Chen, J. G. Analytis, J.-H. Chu, Z. K. Liu, S.-K. Mo, X. L. Qi, H. J. Zhang, D. H. Lu, X. Dai, Z. Fang, S. C. Zhang, I. R. Fisher, Z. Hussain, and Z.-X. Shen, *Science* **325**, 178 (2009).
- [47] L. Fu, *Phys. Rev. Lett.* **103**, 266801 (2009).
- [48] See Supplemental Material at XXX for a detailed derivation of the linear spin polarization, nonlinear current, and nonlinear spin polarization.
- [49] J.-Y. Li, R.-Q. Wang, M.-X. Deng, and M. Yang, *Phys. Rev. B* **99**, 155139 (2019).
- [50] H. Li, H. Gao, L. P. Zârbo, K. Výborný, X. Wang, I. Garate, F. Doğan, A. Čejchan, J. Sinova, T. Jungwirth, and A. Manchon, *Phys. Rev. B* **91**, 134402 (2015).
- [51] V. P. Amin, J. Zemen, and M. D. Stiles, *Phys. Rev. Lett.* **121**, 136805 (2018).
- [52] S. Iihama, T. Taniguchi, K. Yakushiji, A. Fukushima, Y. Shiota, S. Tsunegi, R. Hiramatsu, S. Yuasa, Y. Suzuki, and H. Kubota, *Nat. Electron.* **1**, 120 (2018).
- [53] G. Okano, M. Matsuo, Y. Ohnuma, S. Maekawa, and Y. Nozaki, *Phys. Rev. Lett.* **122**, 217701 (2019).
- [54] C. Safranski, E. A. Montoya, and I. N. Krivorotov, *Nat. Nanotechnol.* **14**, 27 (2019).
- [55] N. Okuma and K. Nomura, *Phys. Rev. B* **95**, 115403 (2017).
- [56] N. Nagaosa, J. Sinova, S. Onoda, A. H. MacDonald, and N. P. Ong, *Rev. Mod. Phys.* **82**, 1539 (2010).
- [57] J. Sinova, D. Culcer, Q. Niu, N. A. Sinitsyn, T. Jungwirth, and A. H. MacDonald, *Phys. Rev. Lett.* **92**, 126603 (2004).
- [58] Y. D. Glinka, S. Babakiray, T. A. Johnson, A. D. Bristow, M. B. Holcomb, and D. Lederman, *App. Phys. Lett.* **103**, 151903 (2013).
- [59] K. Kuroda, M. Arita, K. Miyamoto, M. Ye, J. Jiang, A. Kimura, E.E. Krasovskii, E.V. Chulkov, H. Iwasawa, T. Okuda, K. Shimada, Y. Ueda, H. Namatame, and M. Taniguchi, *Phys. Rev. Lett.* **105**, 076802 (2010).

**Supplementary material to**  
**“Non-linear antidamping spin-orbit torque originating from intra-band transport on the warped surface of a topological insulator”**

PACS numbers:  
Keywords:

**A. DERIVATION OF THE LINEAR SPIN POLARIZATION**

The  $n$ -th order nonequilibrium distribution function derived from the Eq. (2) of the main text can be rewritten as

$$f^{(1)}(\varepsilon_{\mathbf{k}}^{\chi}) = e\gamma \mathbf{E} \cdot \mathbf{v} \frac{\partial f^{(0)}(\varepsilon_{\mathbf{k}}^{\chi})}{\partial \varepsilon_{\mathbf{k}}^{\chi}}, \quad (\text{A.1})$$

$$f^{(2)}(\varepsilon_{\mathbf{k}}^{\chi}) = \frac{e^2 \gamma^2}{\hbar} \left[ \mathbf{E} \cdot \frac{\partial(\mathbf{E} \cdot \mathbf{v})}{\partial \mathbf{k}} \frac{\partial f^{(0)}(\varepsilon_{\mathbf{k}}^{\chi})}{\partial \varepsilon_{\mathbf{k}}^{\chi}} + \hbar(\mathbf{E} \cdot \mathbf{v})^2 \frac{\partial^2 f^{(0)}(\varepsilon_{\mathbf{k}}^{\chi})}{\partial (\varepsilon_{\mathbf{k}}^{\chi})^2} \right]. \quad (\text{A.2})$$

where  $\mathbf{v} = \frac{1}{\hbar} \partial_{\mathbf{k}} \varepsilon_{\mathbf{k}}^{\chi}$  is the group velocity of electrons and an in-plane electric field  $\mathbf{E} = (E_x, E_y)$  is applied. For convenience, we choose a positive Fermi energy (i.e.,  $\varepsilon_F > 0$  lies in the upper band  $\chi = 1$ ). According to the eigenvalues  $\varepsilon_{\mathbf{k}}^{\chi}$  shown in the Eq. (4) of the main text, the group velocity  $\mathbf{v} = (v_x, v_y)$  can be easily solved as

$$\begin{aligned} v_x &= \frac{1}{\hbar \varepsilon_{\mathbf{k}}^+} [\hbar v_F (\hbar v_F k_x - J m_y) + 3\lambda (k_x^2 - k_y^2) \Lambda_{\mathbf{k}}], \\ v_y &= \frac{1}{\hbar \varepsilon_{\mathbf{k}}^+} [\hbar v_F (\hbar v_F k_y + J m_x) - 6\lambda k_x k_y \Lambda_{\mathbf{k}}]. \end{aligned} \quad (\text{A.3})$$

One can calculate the spin polarization using the following formula

$$\mathbf{S}^{oc} = \sum_{\chi} \frac{d^d \mathbf{k}}{(2\pi)^d} \mathbf{s}_{\chi}(\mathbf{k}) \delta f(\varepsilon_{\mathbf{k}}^{\chi}), \quad (\text{A.4})$$

where  $\delta f(\varepsilon_{\mathbf{k}}^{\chi}) = f(\varepsilon_{\mathbf{k}}^{\chi}) - f^{(0)}(\varepsilon_{\mathbf{k}}^{\chi})$  and  $\mathbf{s}_{\chi}(\mathbf{k}) = (\hbar/2) \langle \Psi_{\mathbf{k}}^{\chi} | \boldsymbol{\sigma} | \Psi_{\mathbf{k}}^{\chi} \rangle$  is the spin expectation. Diagonalizing the Hamiltonian of Eq. (3) of the main text, the corresponding eigenstates can be solved as

$$\begin{aligned} |\Psi_{\mathbf{k}}^+\rangle &= [\cos(\xi/2), e^{i\eta} \sin(\xi/2)]^T, \\ |\Psi_{\mathbf{k}}^-\rangle &= [-\sin(\xi/2), e^{i\eta} \cos(\xi/2)]^T, \end{aligned} \quad (\text{A.5})$$

with  $\cos(\xi) = \Lambda_{\mathbf{k}}/\varepsilon_{\mathbf{k}}^+$  and  $\tan(\eta) = (J m_y - \hbar v_F k_x)/(J m_x + \hbar v_F k_y)$ . Using the above eigenstates, one can calculate the spin expectation  $\mathbf{s}_+(\mathbf{k}) = (s_x, s_y, s_z)$  as

$$\mathbf{s}_+(\mathbf{k}) = \left( \frac{J \hbar m_x + \hbar^2 v_F k_y}{2\varepsilon_{\mathbf{k}}^+}, \frac{J \hbar m_y - \hbar^2 v_F k_x}{2\varepsilon_{\mathbf{k}}^+}, \frac{\hbar \lambda k_x^3 - 3 \hbar \lambda k_x k_y^2 + \hbar J m_z}{2\varepsilon_{\mathbf{k}}^+} \right). \quad (\text{A.6})$$

Substituting Eqs. (A.1) and (A.6) to the spin polarization  $\mathbf{S}^{oc}$  of Eq. (A.4) and expanding the integrand of Eq. (A.4) to the second-order term of  $\mathbf{m}$  and  $\lambda$ , one can obtain the results for the linear spin polarization  $\mathbf{S}^{oc(1)}$ , which reads

$$\begin{aligned} S_x^{oc(1)} &= \frac{e\gamma}{8\pi} \left[ \frac{\varepsilon_F}{\hbar v_F} - \frac{1}{6} a_2 \varepsilon_F^2 - a_0 J^2 m_z^2 - \frac{3}{2} a_2 J^2 (m_x^2 + m_y^2 - m_z^2) \right] E_y, \\ S_y^{oc(1)} &= \frac{e\gamma}{8\pi} \left[ -\frac{\varepsilon_F}{\hbar v_F} + \frac{1}{6} a_2 \varepsilon_F^2 + a_0 J^2 m_z^2 + \frac{3}{2} a_2 J^2 (m_x^2 + m_y^2 - m_z^2) \right] E_x, \\ S_z^{oc(1)} &= \frac{e\gamma J^2}{8\pi} \{ [a_1 (-m_x^2 + m_y^2) - 3a_2 m_y m_z] E_x + (2a_1 m_x m_y + 3a_2 m_x m_z) E_y \}, \end{aligned} \quad (\text{A.7})$$

where  $a_0 = 1/(\hbar v_F \varepsilon_F)$ ,  $a_1 = 3\lambda \varepsilon_F / (\hbar^4 v_F^4)$ , and  $a_2 = 3\lambda^2 \varepsilon_F^3 / (\hbar^7 v_F^7)$ . As shown above, all components of the linear spin polarization are even function of  $\mathbf{m}$ . Thus, the linear spin polarization  $\mathbf{S}^{oc(1)}$  only contributes to the field-like SOT.

## B. DERIVATION OF THE NONLINEAR CURRENT

For a positive Fermi energy, the charge current density can be calculated by

$$\mathbf{j} = -e \int \frac{d^d \mathbf{k}}{(2\pi)^d} \mathbf{v}_k f(\varepsilon_{\mathbf{k}}^+). \quad (\text{B.1})$$

Considering the linear response theory, i.e., substituting Eqs. (A.1) and (A.3) into the above equation, the linear current density  $\mathbf{j}^{(1)}$  in FM/TI can be easily solved after some algebraic calculations. The resulting  $\mathbf{j}^{(1)}$  reads as

$$\begin{aligned} \mathbf{j}^{(1)} &= \sigma_D \mathbf{E}, \\ &= \frac{e^2 \gamma \varepsilon_F}{4\pi \hbar^2} \mathbf{E}. \end{aligned} \quad (\text{B.2})$$

For the nonlinear response, one can substitute the non-equilibrium distribution function  $f_{k,\chi}^{(2)}$  of Eq. (A.2) to Eq. (B.1). Following the similar algebraic calculations, the nonlinear current density  $\mathbf{j}^{(2)} = (j_x^{(2)}, j_y^{(2)})$  can be obtain

$$\begin{aligned} j_x^{(2)} &= c_1 (2m_x E_x E_y - 3m_y E_x^2 - m_y E_y^2) - c_2 m_z (E_x^2 - E_y^2), \\ j_y^{(2)} &= c_1 (m_x E_x^2 - 2m_y E_x E_y + 3m_x E_y^2) + 2c_2 m_z E_x E_y, \end{aligned} \quad (\text{B.3})$$

where  $c_1 = 3e^3 \gamma^2 \lambda^2 J \varepsilon_F^3 / (4\pi \hbar^8 v_F^5)$ ,  $c_2 = 3e^3 \gamma^2 \lambda J \varepsilon_F / (8\pi \hbar^5 v_F^2)$ . As shown above,  $\mathbf{j}^{(2)} = 0$  when  $\lambda \rightarrow 0$ .

## C. DERIVATION OF THE NONLINEAR SPIN POLARIZATION

In this section, we discuss in detail the generation of the nonlinear spin polarization. To facilitate the analysis, we need to expand  $\mathbf{s}(\mathbf{k})$  and  $f^{(2)}(\varepsilon_{\mathbf{k}}^+)$  to the second-order term of  $\mathbf{m}$  (or the equivalent  $J$ ), i.e.,  $\mathbf{s}(\mathbf{k}) = \sum_{i=0,1,2} \mathbf{s}^i(\mathbf{k}) J^i$  and  $f^{(2)}(\varepsilon_{\mathbf{k}}^+) = \sum_{i=0,1,2} f_i^{(2)}(\mathbf{k}) J^i$ .

For the convenience of discussions, we here simply set the electric field as  $\mathbf{E} = (E_x, 0)$ . For arbitrary direction of electric field, the case is similar. In the weak warping limit,  $\mathbf{s}^i(\mathbf{k})$  and  $f_i^{(2)}(\mathbf{k})$  can be expand to the second-order term of  $\lambda$ , which is enough to capture the warping effect. In this way, one can obtain the analytical expressions of  $\mathbf{s}^i$  and  $f_i^{(2)}$ ,  $\mathbf{s}(\mathbf{k})$  reads as

$$\begin{aligned} \mathbf{s}^0(\mathbf{k}) &= \left( \frac{\hbar^2 v_F k_y}{2\varepsilon_0}, -\frac{\hbar^2 v_F k_x}{2\varepsilon_0}, \frac{\hbar \lambda k_x^3 - 3\hbar \lambda k_x k_y^2}{2\varepsilon_0} \right), \\ \mathbf{s}^1(\mathbf{k}) &= \left( \frac{\hbar \varepsilon_0 m_x - \hbar^2 v_F k_y \kappa_3}{2\varepsilon_0^2}, \frac{\hbar \varepsilon_0 m_y + \hbar^2 v_F k_x \kappa_3}{2\varepsilon_0^2}, \frac{\hbar \varepsilon_0 m_z - \hbar \lambda k_x^3 \kappa_3 + 3\hbar \lambda k_x k_y^2 \kappa_3}{2\varepsilon_0^2} \right), \\ \mathbf{s}^2(\mathbf{k}) &= \left[ \frac{\hbar^2 v_F k_y (3\kappa_3^2 - \mathbf{m}^2) - 2\hbar \varepsilon_0 m_x \kappa_3}{2\varepsilon_0^3}, \frac{-\hbar^2 v_F k_x (3\kappa_3^2 - \mathbf{m}^2) + 2\hbar \varepsilon_0 m_y \kappa_3}{2\varepsilon_0^3}, \frac{\hbar \lambda (k_x^3 - 3k_x k_y^2) (3\kappa_3^2 - \mathbf{m}^2) - 2\hbar \varepsilon_0 m_z \kappa_3}{2\varepsilon_0^3} \right], \end{aligned}$$

where  $\varepsilon_0 = \sqrt{\lambda^2 (k_x^3 - 3k_x k_y^2)^2 + (\hbar v_F k)^2}$  and  $\kappa_3 = [(k_x^3 - 3k_x k_y^2) \lambda m_z + \hbar v_F (k_y m_x - k_x m_y)] / \varepsilon_0$ . It is found that  $\mathbf{s}^{0,2}(\mathbf{k})$  is odd in  $\mathbf{k}$  while  $\mathbf{s}^1(\mathbf{k})$  is even.



$f_i^{(2)}$  reads as

$$\begin{aligned}
f_0^{(2)} &= \frac{e^2 \gamma^2 E_x^2}{\hbar} \left[ \frac{\kappa_4 - \hbar^2 \kappa_5^2}{\hbar \varepsilon_0} \frac{-b e^{b(\varepsilon_0 - \varepsilon_F)}}{(1 + e^{b(\varepsilon_0 - \varepsilon_F)})^2} + \hbar \kappa_5^2 \frac{b^2 e^{b(\varepsilon_0 - \varepsilon_F)} [e^{b(\varepsilon_0 - \varepsilon_F)} - 1]}{[1 + e^{b(\varepsilon_0 - \varepsilon_F)}]^3} \right], \\
f_1^{(2)} &= \frac{e^2 \gamma^2 E_x^2}{\hbar} \left\{ \frac{3\hbar \kappa_3 \kappa_5^2 - \hbar \kappa_3 \kappa_4 - 2\hbar \kappa_5 (3\lambda(k_x^2 - k_y^2)m_z - \hbar v_F m_y) + 6\lambda k_x \varepsilon_0 m_z}{\hbar \varepsilon_0^2} \times \frac{-b e^{b(\varepsilon_0 - \varepsilon_F)}}{(1 + e^{b(\varepsilon_0 - \varepsilon_F)})^2} \right. \\
&\quad + \frac{\kappa_4 - \hbar^2 \kappa_5^2}{\hbar \varepsilon_0} \times \frac{b^2 e^{b(\varepsilon_0 - \varepsilon_F)} [-1 + e^{b(\varepsilon_0 - \varepsilon_F)}] \kappa_3}{[1 + e^{b(\varepsilon_0 - \varepsilon_F)}]^3} \\
&\quad + \frac{2\kappa_5 [3\lambda(k_x^2 - k_y^2)m_z - \hbar v_F m_y] - 2\hbar \kappa_3 \kappa_5^2}{\varepsilon_0} \times \frac{b^2 e^{b(\varepsilon_0 - \varepsilon_F)} [e^{b(\varepsilon_0 - \varepsilon_F)} - 1]}{[1 + e^{b(\varepsilon_0 - \varepsilon_F)}]^3} \\
&\quad \left. - \hbar \kappa_5^2 \times \frac{b^3 e^{b(\varepsilon_0 - \varepsilon_F)} [1 - 4e^{b(\varepsilon_0 - \varepsilon_F)} + e^{2b(\varepsilon_0 - \varepsilon_F)}] \kappa_3}{[1 + e^{b(\varepsilon_0 - \varepsilon_F)}]^4} \right\}, \\
f_2^{(2)} &= \frac{e^2 \gamma^2 E_x^2}{\hbar} \left\{ \frac{3\hbar^2 (5\kappa_3^2 + \mathbf{m}^2) \kappa_5^2 + 12\hbar^2 \kappa_3 \kappa_5 [3\lambda(k_x^2 - k_y^2)m_z - \hbar v_F m_y] - 2 [3\lambda(k_x^2 - k_y^2)m_z - \hbar v_F m_y]^2 + 3\kappa_3^2 \kappa_4 \varepsilon_0}{\hbar \varepsilon_0^3} \right. \\
&\quad \left. - \frac{b e^{b(\varepsilon_0 - \varepsilon_F)}}{(1 + e^{b(\varepsilon_0 - \varepsilon_F)})^2} + 2 \frac{3\hbar \kappa_3 \kappa_5^2 - \hbar \kappa_3 \kappa_4 - 2\hbar \kappa_5 [3\lambda(k_x^2 - k_y^2)m_z - \hbar v_F m_y] + 6\lambda k_x \varepsilon_0 m_z}{\hbar \varepsilon_0^2} \times \frac{\kappa_3 b^2 e^{b(\varepsilon_0 - \varepsilon_F)} [-1 + e^{b(\varepsilon_0 - \varepsilon_F)}]}{[1 + e^{b(\varepsilon_0 - \varepsilon_F)}]^3} \right. \\
&\quad + \frac{\kappa_4 - \hbar^2 \kappa_5^2}{\hbar \varepsilon_0} \left[ \frac{b^2 e^{b(\varepsilon_0 - \varepsilon_F)} [1 - e^{b(\varepsilon_0 - \varepsilon_F)}] (\kappa_3^2 - \mathbf{m}^2)}{[1 + e^{b(\varepsilon_0 - \varepsilon_F)}]^3 \varepsilon_0} - \frac{\kappa_3^2 b^3 e^{b(\varepsilon_0 - \varepsilon_F)} [1 - 4e^{b(\varepsilon_0 - \varepsilon_F)} + e^{2b(\varepsilon_0 - \varepsilon_F)}]}{[1 + e^{b(\varepsilon_0 - \varepsilon_F)}]^4} \right] \\
&\quad + \hbar \left[ \frac{2(4\kappa_3^2 - \mathbf{m}^2) \kappa_5^2}{\varepsilon_0^2} - \frac{8\kappa_3 \kappa_5 [3\lambda(k_x^2 - k_y^2)m_z - \hbar v_F m_y]}{\hbar \varepsilon_0^2} + \frac{2 [3\lambda(k_x^2 - k_y^2)m_z - \hbar v_F m_y]^2}{\hbar^2 \varepsilon_0^2} \right] \frac{b^2 e^{b(\varepsilon_0 - \varepsilon_F)} [e^{b(\varepsilon_0 - \varepsilon_F)} - 1]}{[1 + e^{b(\varepsilon_0 - \varepsilon_F)}]^3} \\
&\quad + 2 \frac{2\kappa_5 [3\lambda(k_x^2 - k_y^2)m_z - \hbar v_F m_y] - 2\hbar \kappa_3 \kappa_5^2}{\varepsilon_0} \times \frac{\kappa_3 b^3 e^{b(\varepsilon_0 - \varepsilon_F)} [1 - 4e^{b(\varepsilon_0 - \varepsilon_F)} + e^{2b(\varepsilon_0 - \varepsilon_F)}]}{[1 + e^{b(\varepsilon_0 - \varepsilon_F)}]^4} \\
&\quad + \hbar \kappa_5^2 \left[ \frac{\kappa_3^2 b^4 e^{b(\varepsilon_0 - \varepsilon_F)} [-1 + 11e^{b(\varepsilon_0 - \varepsilon_F)} - 11e^{2b(\varepsilon_0 - \varepsilon_F)} + e^{3b(\varepsilon_0 - \varepsilon_F)}]}{[1 + e^{b(\varepsilon_0 - \varepsilon_F)}]^5} \right. \\
&\quad \left. + \frac{b^3 e^{b(\varepsilon_0 - \varepsilon_F)} [1 - 4e^{b(\varepsilon_0 - \varepsilon_F)} + e^{2b(\varepsilon_0 - \varepsilon_F)}] (\kappa_3^2 - \mathbf{m}^2)}{[1 + e^{b(\varepsilon_0 - \varepsilon_F)}]^4 \varepsilon_0} \right] \left. \right\},
\end{aligned}$$

where  $\kappa_4 = (15k_x^4 - 36k_x^2 k_y^2 + 9k_y^4)\lambda^2 + (\hbar v_F)^2$  is even in  $\mathbf{k}$  and  $\kappa_5 = [(3k_x^5 - 12k_x^3 k_y^2 + 9k_x k_y^4)\lambda^2 + (\hbar v_F)^2 k_x] / (\hbar \varepsilon_0)$  is odd in  $\mathbf{k}$ , and  $b = 1/(k_B T)$ . It is found that  $f_{0,2}^{(2)}(\mathbf{k})$  is even in  $\mathbf{k}$  while  $f_1^{(2)}(\mathbf{k})$  is odd in  $\mathbf{k}$ .

All the above results indicate that the nonzero integrand terms of  $\mathbf{k}$  in  $\mathbf{S}^{oc(2)}$  are  $\mathbf{s}^0(\mathbf{k}) \cdot f_1^{(2)}(\mathbf{k})$  and  $\mathbf{s}^1(\mathbf{k}) \cdot f_0^{(2)}(\mathbf{k})$ .